

High-Power Picosecond Pulse Generation Due to Mode-Locking With a Monolithic 10-mm-Long Four-Section DBR Laser at 920 nm

S. Schwertfeger, A. Klehr, A. Liero, G. Erbert, and G. Tränkle

Abstract—A 10-mm-long four-section distributed Bragg reflector laser with a double-quantum-well heterostructure at 920 nm was realized. A maximum optical pulse power of 3.6 W with a repetition rate of 4.1 GHz corresponding to the laser length was reached. The full-width at half-maximum of the pulses was 7 ps measured with an autocorrelator. A maximum pulse energy of 25 pJ was reached.

Index Terms—Distributed Bragg reflector (DBR) laser, high power, mode locking, picosecond (ps) pulse.

I. INTRODUCTION

HIGH-POWER optical pulses with a small spectral linewidth and a repetition rate of few gigahertz (GHz) are required for several applications, e.g., fiber communications, display technique, or optical communications [1]. Typically, high-power pulses are generated by mode-locked solid state lasers. The main drawbacks of such systems are their large dimensions and high cost. Semiconductor lasers, on the other hand, offer the advantage of small size, high efficiency, and low cost.

Mode-locking can be realized either in external cavities or in monolithic lasers through different approaches [2]–[4]. For repetition rates up to several GHz, external cavities are commonly used owing to the high round-trip time needed. Monolithic cavity mode locked lasers, in contrast, offer the advantage of being very compact and do not exhibit mechanical instabilities associated with the optical elements required in an external cavity. Typically these devices can generate pulses with repetition frequencies of several tens of GHz [5]. Despite the need of long cavities, monolithic mode-locked lasers for smaller repetition frequencies were investigated too [6].

In this letter, we report on passive mode-locking experiments on a 10-mm-long four-section distributed Bragg reflector (DBR) laser. A theoretical analysis of such devices at a wavelength of 1060 nm was published in 2005 by Hasler *et al.* [7].

II. DEVICE STRUCTURES AND EXPERIMENTAL SETUP

The laser was grown by low-pressure metal–organic vapor phase epitaxy in two steps, similarly as described in [8] and

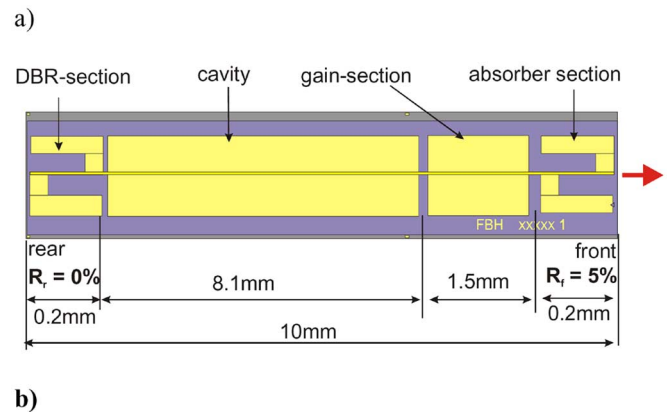
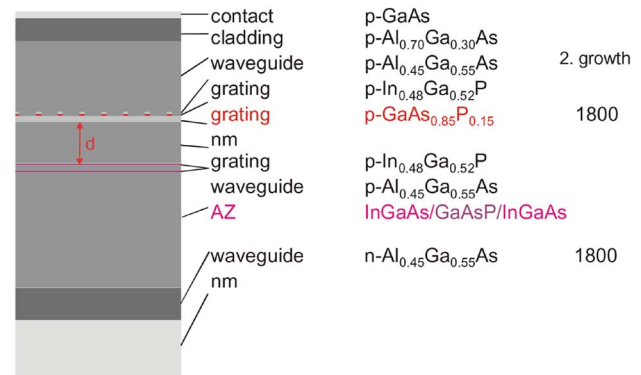


Fig. 1. (a) Vertical layer structure. (b) Scheme of the four-section DBR laser.

[9]. The first growth step consisted of a n-GaAs buffer, n-Al_{0.70}Ga_{0.30}As cladding, 1800-nm n-Al_{0.45}Ga_{0.55}As waveguide, an active InGaAs double-quantum-well embedded in GaAsP spacer layers, a 200-nm first part of the p-Al_{0.45}Ga_{0.55}As waveguide, and an InGaP–GaAs–InGaP layer sequence in which the grating is formed in the Bragg section by holographic photolithography using a frequency-quadrupled Nd-YAG laser and wet-chemical etching. In order to obtain a lasing wavelength of 920 nm, the period of the second-order grating was adjusted to 282 nm. A coupling coefficient of about 63 cm⁻¹ was determined by fitting amplified spontaneous emission spectra measured below threshold to a parameterized theoretical model [10]. The grating structure is overgrown in a second epitaxial step with the remainder 1600-nm p-Al_{0.45}Ga_{0.55}As waveguide layer, a p-Al_{0.70}Ga_{0.30}As cladding, and the highly doped p-GaAs contact layer [see Fig. 1(a)]. Lateral optical confinement and

Manuscript received May 24, 2007; revised August 10, 2007.

The authors are with the Ferdinand-Braun-Institut für Höchstfrequenztechnik (FBH), D-12489 Berlin, Germany (e-mail: sven.schwertfeger@fbh-berlin.de).

Color versions of one or more of the figures in this letter are available online at <http://ieeexplore.ieee.org>.

Digital Object Identifier 10.1109/LPT.2007.908649

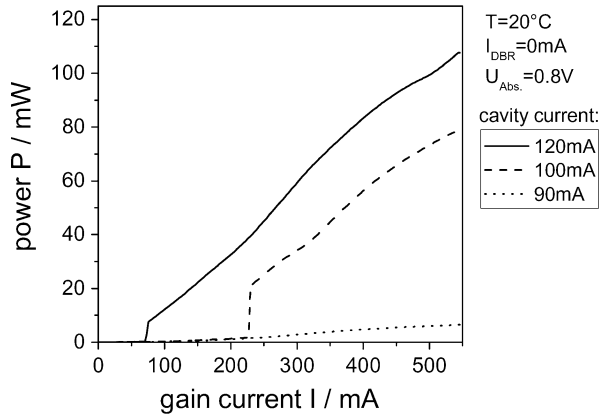


Fig. 2. Typical P - I characteristic for different cavity currents.

p-contacting is provided by a ridge waveguide (RW) structure. The four-section DBR laser as investigated experimentally is depicted in Fig. 1(b). It consists of a gain section of $1500 \mu\text{m}$, a cavity section of $8100 \mu\text{m}$, a DBR section of $200 \mu\text{m}$, and an absorber section of $200\text{-}\mu\text{m}$ length, respectively. The layout of the evaporated p-metallization allows electrically separated contacts for the four sections, where the epitaxial structure for these sections is the same and the active layer extends over the whole length. The total length of the four-section DBR laser is 10 mm , corresponding to a round-trip time of 243 ps .

The width of the ridge is about $2 \mu\text{m}$, in order to attain fundamental mode emission. Due to the superlarge optical cavity of the waveguide layers, the vertical far-field has a full-width at half-maximum (FWHM) angle of $\Theta_{\perp} = 19^{\circ}$. The lateral far-field FWHM angle $\Theta_{\parallel} = 7^{\circ}$. The rear facet formed by the DBR section is antireflection coated to $R = 10^{-4}$. The front facet formed by the absorber has a reflectivity of 5% . The RWs of the absorber and DBR sections are covered with very narrow TiPtAu metal stripes for a selective heating due to an additional current through the ohmic contacts.

The devices were mounted p-up on an CuW submount and attached to a temperature-controlled copper heat sink.

For the measurements, all sections were biased with a dc current. Absorption in the DBR and absorber sections can be increased by applying a current through the surface heaters on the top of the respective sections. In our case, reverse bias was applied to the absorber section in order to achieve higher absorption. The pulse length was measured by coupling the light into an APE pulse check 150 autocorrelator. The power-current (P - I) characteristics were measured with a 90-s-long triangular ramp using an oscilloscope and a photodiode. For spectra and RF measurements, the emitted light was coupled into an optical fiber, using an aspheric lens and a 40-dB optical isolator.

III. RESULTS

Fig. 2 shows typical P - I characteristics for the four-section DBR laser. The current through the gain section I_{gain} was increased continuously for different cavity currents I_{cav} . The DBR section was not biased and the absorber section was reverse biased with $U_{\text{abs}} = -0.8 \text{ V}$. For a cavity current lower than $I_{\text{cav}} = 90 \text{ mA}$, no lasing operation was observed, which can be explained by a high absorption in the cavity section. The

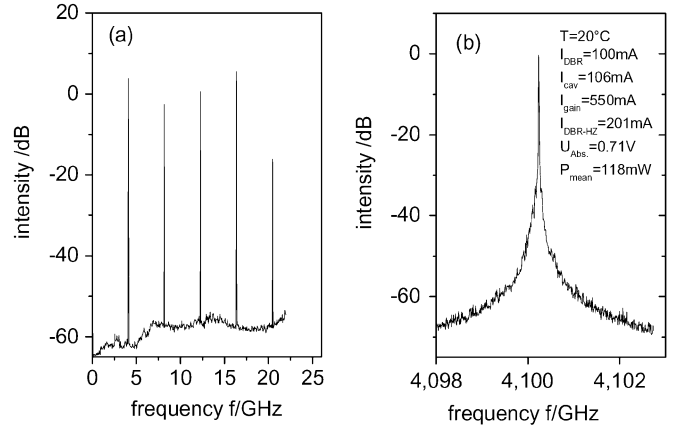


Fig. 3. (a) RF spectrum for high-power passive mode-locking and (b) the 4.1-GHz line with higher resolution.

cavity current density was lower than the transparency current density for this section. For $I_{\text{cav}} = 100 \text{ mA}$ and a gain current of $I_{\text{gain}} = 230 \text{ mA}$, an abrupt switch ON of lasing could be seen. If the current was further increased, the P - I characteristic showed the typical behaviour for semiconductor laser diodes. For higher cavity currents, the threshold current decreased and the abrupt start of lasing vanished, but the emission power was much higher.

To investigate mode-locking, RF power spectra with a 25-GHz fast Si photodiode coupled to a 30-dB amplifier and an FSEK 30 Rhode and Schwarz RF Analyzer were measured. In these investigation, the gain current I_{gain} , the current through the DBR section I_{DBR} , the cavity current I_{cav} , the reverse bias of the absorber section U_{abs} , and the heating currents of the DBR section $I_{\text{DBR,heat}}$ and absorber section $I_{\text{abs,heat}}$ were varied. For a wide variation of these parameters, passive mode-locking was observed.

Especially the DBR section current and DBR heating current influenced the pulse shape, pulse length, and emission wavelength, as well as power, while all other parameters were kept constant. The mean power compared to an unbiased DBR section could be increased about 35 mW . The autocorrelation pulse length FWHM varied in a range from 10 to 22 ps . This behaviour could be attributed to the change in reflection profile of the DBR section by application of a current.

An RF spectrum, at $I_{\text{gain}} = 550 \text{ mA}$, $I_{\text{cav}} = 106 \text{ mA}$, and $I_{\text{DBR}} = 100 \text{ mA}$, is presented in Fig. 3. The absorber section was reverse biased with 0.71 V . The DBR section was selectively heated with $I_{\text{DBR,heat}} = 201 \text{ mA}$. In Fig. 3(a), a sharp lines at the round-trip frequency of 4.1 GHz and its higher harmonics can be seen. Fig. 3(b) shows the RF spectrum at 4.1 GHz with higher resolution. With these parameters, the highest mean optical output power of $P = 118 \text{ mW}$ at short pulse length was reached.

The autocorrelation function under the same conditions is shown in Fig 4. The dashed line shows the sech^2 fit function. A sharp main peak with an FWHM of about $\tau = 10.4 \text{ ps}$ is measured. Assuming a sech^2 pulse shape yields a corresponding pulse length of $\tau = 7.0 \text{ ps}$. Between 30 – 55 ps and 100 – 120 ps , small sidelobes with an intensity $< 5\%$ can be seen. This implies

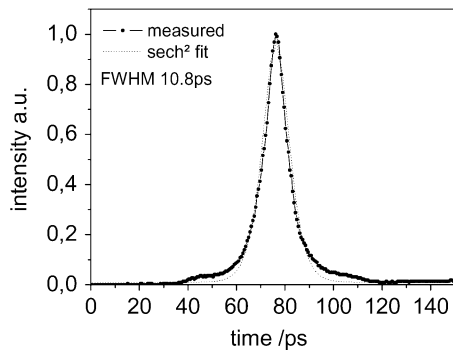


Fig. 4. Autocorrelation function of the mode-locked pulses at 4.1 GHz.

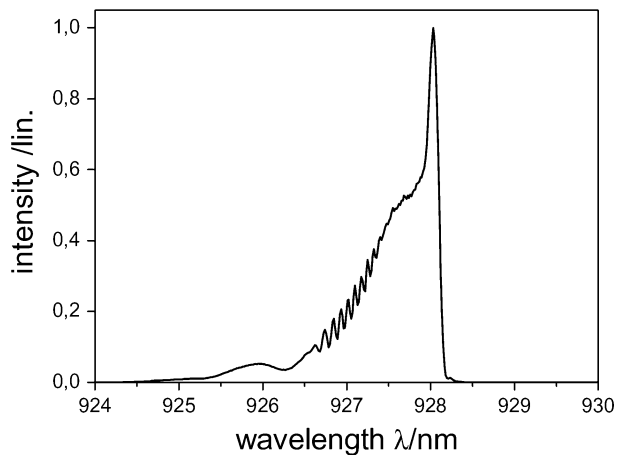


Fig. 5. Time averaged spectrum of a passive mode-locked multisection laser.

that there is a small peak close to the main peak. The calculated peak pulse power is 3.6 W with an overall pulse energy of 25 pJ.

A spectrum averaged over many pulses is shown in Fig. 5 on a linear scale. The FWHM is 1.7×10^{11} Hz. The resulting time-bandwidth product $\Delta\nu \cdot \Delta\tau$ is calculated to be 1.2. It is hence almost four times larger than a bandwidth limited sech^2 shaped pulse. Therefore, it shows a significant chirp, but for

pulse peak power low as 500 mW, a nearly bandwidth limited pulse ($\Delta\nu \cdot \Delta\tau = 0.44$) was observed. The increasing chirp with increasing power is broadly attributed to higher self-phase modulation [11].

IV. SUMMARY

First results on monolithic 10-mm-long four-section 920-nm InGaAs passively mode-locked laser have been presented. Stable mode-locking at the ground mode was observed, with a minimal pulse length of 7 ps. A high pulse peak power of 3.6 W was reached.

REFERENCES

- [1] K. Williams, M. G. Thompson, and I. White, "Long-wavelength monolithic mode-locked diode lasers," *New J. Phys.*, vol. 6, pp. 179-1-179-30, 2004, article 179.
- [2] D. J. Derickson, R. J. Helkey, A. Mar, J. A. Karin, J. G. Wasserbauer, and J. E. Bowers, "Short pulse generation using multisection mode-locked semiconductor lasers," *IEEE J. Quantum Electron.*, vol. 28, no. 10, pp. 2186-2202, Oct. 1992.
- [3] E. Kapon, Ed., *Semiconductor Lasers I: Fundamentals*. San Diego, CA, London, U.K.: Academic, 1999, pp. 269-280.
- [4] U. Keller and A. C. Tropper, Passively modelocked surface-emitting semiconductor lasers Physics Report 429, 2006, pp. 67-120.
- [5] R. Kaiser, B. Hüttle, H. Heinrich, S. Fidorra, W. Rehbein, H. Stolpe, W. Ebert, and G. Sahin, "Tunable monolithic mode-locked lasers on InP with low timing jitter," *IEEE Photon. Technol. Lett.*, vol. 15, no. 5, pp. 634-636, May 2003.
- [6] P. B. Hansen, G. Rayborn, U. Koren, B. I. Miller, M. G. Young, M. A. Newkirk, M.-D. Chien, B. Tell, and C. A. Burrus, "2 cm long monolithic multisection laser for active modelocking at 2.2 GHz," *Electron. Lett.*, vol. 29, no. 9, pp. 739-741, Apr. 1993.
- [7] K. H. Hasler, A. Klehr, H. Wenzel, and G. Ebert, "Simulation of high-power pulse generation due to modelocking in long multisection lasers," *Proc. Inst. Elect. Eng. Optoelectronics*, vol. 152, no. 2, pp. 77-85, Apr. 2005.
- [8] H. Wenzel *et al.*, "High-power ridge-waveguide distributed-feedback lasers emitting at 860 nm," *Electron. Lett.*, vol. 38, no. 25, pp. 1676-1677, Dec. 2002.
- [9] H. Wenzel *et al.*, "Design and realization of high power DFB lasers," *Proc. SPIE 2005*, vol. 5738, pp. 411-424.
- [10] H. Wenzel, "Green's function based simulation of the optical spectrum of multisection lasers," *IEEE J. Sel. Topics Quantum Electron.*, vol. 9, no. 3, pp. 865-871, May. 2003.
- [11] G. P. Agrawal and N. A. Olsson, "Self-phase modulation and spectral broadening of optical pulses in semiconductor laser amplifiers," *IEEE J. Quantum Electron.*, vol. 25, no. 11, pp. 2297-2306, Nov. 1989.